Modified Fourier–Hankel method based on analysis of errors in Abel inversion using Fourier transform techniques (published, see [1])

Shuiliang Ma, Hongming Gao, and Lin Wu

State Key Laboratory of Advanced Welding Production Technology, Harbin Institute of Technology, Harbin 150001, People's Republic of China

Abstract

Errors in discrete Abel inversion methods using Fourier transform techniques have been analyzed. The Fourier expansion method is very accurate but sensitive to noise. The Fourier–Hankel method has a significant systematic negative deviation, which increases with the radius; inversion error of the method can be reduced by adjusting the value of a factor. With a decrease of the factor both methods show noise filtering property. Based on the analysis, a modified Fourier–Hankel method that is accurate, computationally efficient, and has the ability to filter noise in the inversion process is proposed for applying to experimental data.

1. Introduction

Spatially resolved measurements are important for determining certain physical parameters in many fields of physics and engineering. Unfortunately, in most circumstances, the measured signals are a line-of-sight integration of some quantity. Tomographic techniques are therefore needed for reconstruction of the local values of these parameters from experimental data. Particularly, such as in plasma diagnostics [2] and flame research [3], for a cylindrically symmetric and optically thin radiation source, the radially distributed emission coefficients can be reconstructed from the measured intensities by a method known as Abel inversion.

Abel inversion is an ill-posed problem because of the singularity in the integral at the lower limit, and the derivative of the projection greatly amplifies the noise inherent in the experimental data. These difficulties as well as the discrete form of the values measured make the inversion difficult to be directly applied to experimental data. Therefore, many inversion methods have been developed over the past years. For example, some use spline interpolation techniques [4,5], and some others use polynomial least squares fitting approaches [6–8].

Among these methods, algorithms with the technique of Fourier transform are widely used [9–17]. One approach that performs the inversion by first taking the Fourier transform of the projected data and then following it with the inverse Hankel transform known as the Fourier–Hankel (FH) method has been reported by many researchers [10–17]. It is said that this method can greatly reduce the computation time by using the fast Fourier transform (FFT) algorithm and the singularity in the inverse Abel transform is avoided as the analytical method has been used [11–13]. There are reports that this method can provide higher inversion accuracies than some other methods, even for poorly sampled data [13,14], but there are also results indicating that the FH method yields a rather poor inversion especially for small sets of data [15]. In addition, it is found that this kind of method is more sensitive to noise than other inverse techniques and it produces artificial structures [16]. These phenomena appeared, and a proper explantation cannot be found because little attention has been paid to a special inversion method, the Fourier expansion (FE) method [9,10], which also uses the technique of Fourier transform and is in fact closely related to the FH method.

In this paper, the inversion errors in the FE and FH methods were studied in detail, the disagreement appeared in literature was resolved, and a modified method was proposed. In the following sections, we first describe the two discrete inversion methods using Fourier transform techniques, second we analyze the inversion errors and the noise properties of these methods, and finally we present the modified method with some examples.

Email: shlgma@126.com (Shuiliang Ma).

2. Discrete Abel inversion methods using Fourier transform

For a cylindrically symmetric radiation source with radius R, the relation between the measured intensity $I(x)$ and the emission coefficient $\varepsilon(r)$ is described by the forward Abel transform

$$I(x) = 2\int_x^R (r^2 - x^2)^{-1/2}\varepsilon(r)r\mathrm{d}r, \tag{1}$$

and the reconstruction of the emission coefficient is realized by the inverse Abel transform

$$\varepsilon(r) = -\frac{1}{\pi}\int_r^R (x^2 - r^2)^{-1/2}I'(x)\mathrm{d}x, \tag{2}$$

where $I'(x) = \mathrm{d}I(x)/\mathrm{d}x$.

As the values of the intensity measured are always in sets of discrete data, to take the inversion it is convenient to use a discrete method that directly connects the studied values to the experimentally obtained intensities by a two-dimensional matrix, namely

$$\varepsilon(r_i) = \sum_{j=0}^{n} P_{ij}I(x_j), \tag{3}$$

where n is the number of data at one side of the source, $r_i = i\Delta r$ $(i = 0,1,\ldots,n)$, $x_j = j\Delta x$ $(j = 0,1,\ldots,n)$, and $\Delta r = \Delta x = R/n$; Δr and Δx denote the data spacing. Since for the reconstruction of $\varepsilon(r_i)$ only a single summation is performed, the reconstruction speed will be very fast if the inversion matrix P_{ij} is calculated in advance and the noise filtering process is not considered, which is in fact an important step in the inversion of experimental data that are unavoidably contaminated by noise. Thus the matrix form of the inversion is especially suitable for fast processing of a large amount of data.

2.1. *Fourier expansion method*

The FE method is simplified by Kalal and Nugent [10] according to the work of Tatekura [9], where the technique of expanding the intensity function $I(x)$ as a summation of cosine basis functions was used to perform the Abel inversion. Assuming that the intensity is symmetrically distributed and has zero values outside the radius of the source, $I(x)$ may be expanded as [10]

$$I(x) = a_0 + \sum_{k=1}^{\infty} a_k \cos\left(\frac{k\pi x}{R}\right), \tag{4}$$

where a_k are the Fourier expansion coefficients. By substituting Eq. (4) into Eq. (2) and with some simplifications, we get

$$\varepsilon(r) = \frac{\pi}{2R}\sum_{k=1}^{\infty} k\,a_k\,g(k\pi/R, r, R), \tag{5}$$

where

$$g(\omega, r, R) = \frac{2}{\pi}\int_r^R (x^2 - r^2)^{-1/2}\sin(\omega x)\mathrm{d}x. \tag{6}$$

Note that $g(\omega, r, R) = g(\omega R, r/R, 1)$, thus for convenience we use $g(\omega', r')$ to represent $g(\omega R, r/R, 1)$. This indicates that the radius of the source is normalized to unity.

Eq. (5) is an analytical expression for the Abel inversion. Since a discrete method with an inversion matrix is more attractive, we change it to the matrix form as expressed by Eq. (3), that is

$$\varepsilon(r_i) = \frac{\pi}{2nR}\sum_{k=1}^{n} k\,a(k)\,g(k\pi, i/n), \tag{7}$$

where

$$a(k) = \sum_{j=-n}^{n-1} I(x_j)\cos(\frac{jk\pi}{n}). \tag{8}$$

A potential advantage of the method is that noise filtering can be implemented in the inversion process by controlling the number of expansion terms.

2.2. *Fourier–Hankel method*

The FH method is commonly used in image reconstruction from projections such as fields of plasma diagnostics [11–15] and charged particle imaging [16,17]. It can be transformed in terms of Fourier and Hankel integrals. By taking the Fourier transform of the projected intensity in Eq. (1) and changing the variables of the integration to polar coordinates, it can be shown that the Fourier transform of $I(x)$ is equal to the zero-order Hankel transform of $\varepsilon(r)$. Therefore, the emission coefficient can be recovered from the inverse Hankel transform [10–15]

$$\varepsilon(r) = \frac{1}{2\pi}\int_0^{\infty} G(\omega)\omega J_0(\omega r)\mathrm{d}\omega, \tag{9}$$

where $G(\omega)$ is the continues Fourier transform of the projected intensities, and

$$J_0(\omega r) = \frac{2}{\pi}\int_r^{\infty} (x^2 - r^2)^{-1/2}\sin(\omega x)\mathrm{d}x \tag{10}$$

is the zero-order Bessel function of the first kind [18].

With frequency spacing $\Delta\omega = \alpha\pi/R$, Eq. (9) can be discretized as

$$\varepsilon(r_i) = \frac{\alpha^2\pi}{2nR}\sum_{k=1}^{n} k\,G(\alpha k)J_0(\frac{\alpha ik\pi}{n}), \tag{11}$$

where

$$G(\alpha k) = \sum_{j=-n}^{n-1} I(x_j)\cos(\frac{\alpha jk\pi}{n}). \tag{12}$$

Though this method has been extensively used by many researchers in past years, there are only two kinds of discrete inversion forms that can be found in literature (to the knowledge of the authors). One discrete expression [19] was originally presented by Smith et al. [11], who modified the discrete inverse Hankel transform algorithm of Candel [20], and wrote it into a summation of terms related to the Fourier transform components of the intensity data. Since the FFT algorithm has been used, their formula is similar to Eq. (11) with $\alpha = 1$. The other discrete expression appeared in [14], where $\Delta x\Delta\omega = 1/(2n+1)$ is assumed and the continuous Fourier transform that is discretized as the FFT algorithm cannot be used. This discrete method is equal to Eq. (11) with $\alpha = n/[(2n+1)\pi] \approx 1/(2\pi)$.

3. Error analysis

Simulated data are used to test the performance of the two discrete inversion methods. The simulated intensities and the corresponding emission coefficients are calculated from two pairs of profiles which are widely used in literature to test the performance of different Abel inversion methods. The first pair of test profiles with off-axis peaks in the emission coefficient function that is a common distribution in experimental data are as follows:

$$I_1(x) = \frac{16}{105}(1 - x^2)^{5/2}(19 + 72x^2), \quad 0 \leqslant x \leqslant 1, \tag{13}$$

$$\varepsilon_1(r) = (1 - r^2)^2(1 + 12r^2), \quad 0 \leqslant r \leqslant 1. \tag{14}$$

Profiles with such a characteristic make big challenges for Abel inversion as the values in the area near the center of the source are difficult to be reconstructed. The second pair of test profiles are of a Gaussian type that is also commonly encountered in experimental data but relatively easy to be reconstructed. For this kind of profile, the following expressions taking from [11] are used:

$$I_2(x) = \exp(-x^2/400), \quad 0 \leqslant x \leqslant 100, \tag{15}$$

$$\varepsilon_2(r) = \frac{1}{20\sqrt{\pi}}\exp(-r^2/400), \quad 0 \leqslant r \leqslant 100. \tag{16}$$

For a source with radius R, if we keep the data spacing Δx changeless, extend the radius of the source to R/α ($0 < \alpha < 1$) and assume the emission coefficient in the area $R < r \leqslant R/\alpha$ is zero, with the Fourier components $n+1 \sim n/\alpha$ (i.e., $G(\alpha(n+1)) \sim G(n)$) of the intensities being neglected according to Eq. (5), a discrete inversion formula similar to Eq. (11) can be obtained as

$$\varepsilon(r_i) = \frac{\alpha^2\pi}{2nR}\sum_{k=1}^{n} k\,G(\alpha k)g(k\pi, \alpha i/n). \tag{17}$$

In this sense, the value of α has a straightforward meaning; the parameter of an ideal lowpass filter for controlling the smoothing degree of the data for inversion; with a lower value of α, more Fourier components of the intensities will be dropped.

The similarity between Eqs. (11) and (17) is obvious. Before analyzing the difference we use an example to compare the results inverted with the two methods. Fig. 1 shows the emission coefficients and the corresponding absolute inversion errors calculated from intensity data in Eq. (13) with $n = 10$ and $\alpha = 1$. Huge differences appeared between the results of the two methods; the FE method seems to be very accurate and only has a undetectable uncertainty; while the result inverted with the FH method is completely unacceptable, the inversion error is up to 50% compared to the theoretical emission values. Two trends are easily distinguished, the inversion error of the FH method is systematically negative and becomes larger with an increase of the radius.

The inversion error of the FE method arises from two aspects: the discretization of the continuous Fourier transform and the truncation of the series expansion in Eq. (4). Generally, the discretized Fourier transform will have a high accuracy. If

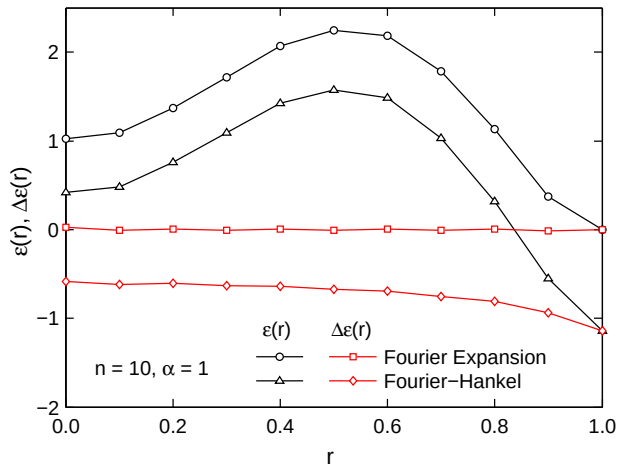

Fig. 1. Radial variations of the emission coefficients and the corresponding absolute errors in the inversion performed with the FE and FH methods.

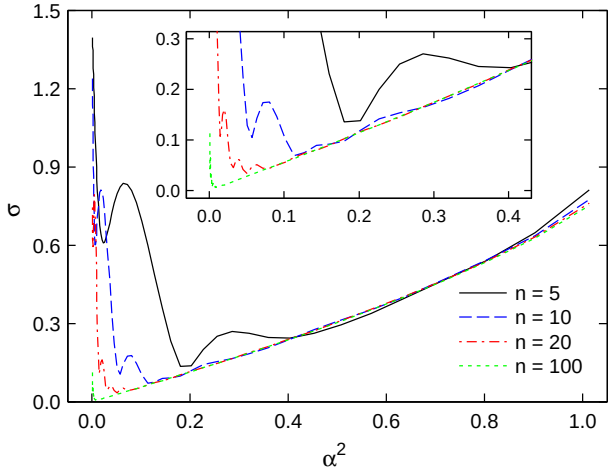

Fig. 2. Variations of the standard deviation σ for the FH method calculated with various values of the number of data n as a function of α^2.

the Nyquist criteria [21] is satisfied, i.e., $\alpha \leqslant 1$, the truncation error will be very small. Thus the FE method is very accurate even for poorly sampled data. However, if noise smoothing is considered the value of α should

not be determined too small, as which will lead to a too low Nyquist frequency and so the inversion error will be increased rapidly since this means that a low cut-off frequency of the ideal lowpass filter has been used, which will seriously distort the original signal. Thus it is clear that, as the decrease of α, the inversion error of the FE method increases. For a proper value of α in the interval $(0,1]$, the error is rather small since in most cases the intensity data can be well approximated by only the first few components of the Fourier frequencies.

For the FH method, however, except for the discretized error of the continuous Fourier transform and that of the inverse Hankel transform in Eq. (9) corresponding to the truncation error of the series expansion in Eq. (4), significant error is caused by the replacement of $g(\omega,r,R)$ by $J_0(\omega r)$.

The difference between the two methods is only related to the two basis functions $g(\omega,r,R)$ and $J_0(\omega r)$. For a certain radial position $r_i = i/n$ of the source with a unity radius, according to Eqs. (6) and (10) we can rewrite $g(\omega,r,R)$ and $J_0(\omega r)$ as

$$g(\omega,r_i) = \frac{2}{\pi}\int_i^n (t^2-i^2)^{-1/2}\sin(\frac{\omega t}{n})\mathrm{d}t, \tag{18}$$

$$J_0(\omega r_i) = \frac{2}{\pi}\int_i^\infty (t^2-i^2)^{-1/2}\sin(\frac{\omega t}{n})\mathrm{d}t. \tag{19}$$

The similarity and difference between the two expressions are evident. It seems that when $n\to\infty$, $g(\omega,r) = J_0(\omega r)$, and so the FE method tends to the FH method as pointed out in [10]. However, it is worth noting that this is misleading and incorrect. Because the radius of the source is unity, when $n\to\infty$, it is also true that $i\to\infty$, so $g(\omega,r)$ will not tend to $J_0(\omega r)$. Thus if the radius of the source is kept constant, an increase in the number of data cannot improve the inversion accuracy of the FH method.

The difference between $g(\omega,r,R)$ and $J_0(\omega r)$ can be expressed as

$$\begin{aligned} f(\omega,r,R) &= J_0(\omega r) - g(\omega,r,R) \\ &= \frac{2}{\pi}\int_R^\infty (x^2-r^2)^{-1/2}\sin(\omega x)\mathrm{d}x. \end{aligned} \tag{20}$$

The relation $f(\omega,r,R) = f(\omega R, r/R, 1)$ is satisfied, so the use of $f(\omega',r')$ also means that the radius of the source is normalized to unity.

From Eq. (20) it can be found that only when the radius of the source tends to infinity, the lower limit in the integral will also tend to infinity and $f(\omega,r,R)\to 0$. Therefore, it is the radius of the source but not the number of inversion data that leads to the difference between the two functions; only by increasing the radius of the source, i.e., decreasing the value of α, will the inversion error of the FH method be reduced.

To validate the conclusions, the standard deviations calculated using the intensity data in Eq. (13) with various values of n and α are plotted in Fig. 2. The standard deviation was estimated using the following equation:

$$\sigma = \left\{\frac{1}{n+1}\sum_{i=0}^{n}\left[\varepsilon_c(r_i)-\varepsilon_t(r_i)\right]^2\right\}^{1/2}, \tag{21}$$

where $\varepsilon_c(r_i)$ and $\varepsilon_t(r_i)$ are the calculated and theoretical emission coefficients at point r_i.

As shown in Fig. 2, for each profile corresponding to one value of n, as the decrease of α the standard deviation first deceases, and when α decreases to a certain value the error then increases rapidly. This tendency is consistent with the previous error analysis. It is clear to see that σ is nearly unchanged for a fixed α with different values of n. This validates that the increase of the number of data cannot improve the inversion accuracy of the FH method. We can also see that σ is almost proportional to α^2 especially for a small α, so the error decreases rather slow. To obtain an acceptable inversion (e.g., $\sigma \leqslant 1\%$), a small α must be chosen (e.g., $\alpha \leqslant 0.2$). Consequently, the FH method can only be applied to large sets of data, as for small values of n the desired accuracy cannot be achieved.

According to Eqs. (11), (17) and (20), the difference between the two methods can be written as

$$\delta(\alpha,r) = \frac{\alpha^2\pi}{2nR}\sum_{k=1}^{n} k\,G(\alpha k)\,f(k\pi,\alpha r). \tag{22}$$

This equation indicates that if the truncation error of the series expansion is small, the inversion error of the FH method mainly arises from $f(k\pi,\alpha r)$; note that the inversion error of the FE method can be neglected compared to this error.

The trend that the error increasing with the radius is related to the property of $f(k\pi,\alpha r)$ as a function of r. As shown in Fig. 3, for different values of k, $f(k\pi,\alpha r)$ increases as r varies from 0 to 1. For the first few terms of k, the value of $f(k\pi,\alpha r)$ is relatively large. Thus there is no surprise that the error in the inversion is huge and increases as radius r becomes larger.

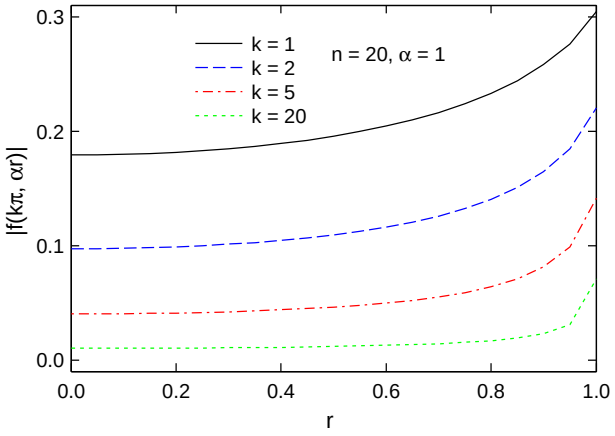

Fig. 3. Radial distributions of the difference $f(k\pi,\alpha r)$ between $J_0(\alpha\omega r)$ and $g(\omega,\alpha r)$ for various values of k calculated with intensities in Eq. (13).

Another trend is the negative error that is caused due to the distributions of $kG(\alpha k)$ and $f(k\pi,\alpha r)$ as functions of k. Both of the functions are oscillatory and decrease with the increase of k, so the summation of their products is mainly determined by the first few terms that are negative as shown in Fig. 4(a). It is evident that the summation of $kG(\alpha k)f(k\pi,\alpha r)$ is negative; therefore the error in the FH method is also negative.

However, for some special distributions of $kG(\alpha k)$ (e.g., there is no oscillation), the inversion error would be very small. One such case is the Gaussian function such as in Eq. (15). As shown in Fig. 4(b), $kG(\alpha k)$ decreases monotonously with the increase of k, thus its product with $f(k\pi,\alpha r)$ is oscillatory as the distribution of $f(k\pi,\alpha r)$ is oscillatory. This leads to a very small summation, and so the inversion error is also very small. This case illustrates that there is no evident error in some tests [11,12] with such kinds of profiles.

4. Noise properties of the methods

For a desirable Abel inversion method, it should be fast, accurate, and stable. The last property is in fact very important as the experimental data inherently contain noise that will greatly deteriorate the inverted result and the filtering of noise in most circumstances is difficult to control. Thus the noise amplification properties of the FE and FH methods are compared and discussed in this section.

Fig. 5(a) shows the theoretical emission coefficients and the results inverted with the two methods. The intensity data were generated from Eq. (13) with the value $I_1(1/2)$ lowered to $0.95I_1(1/2)$ to simulate noise in the experimental data. For the FH method, the inverted distribution is only a little lower in the area near the position of the noise; values at other positions are very consistent with the theoretical ones. This is because a small α was chosen, which leads to a negligible inversion error and the good noise filtering property. The result inverted with the FE method is however greatly affected by the noise. The error was magnified more than five times at the position of the noise; oscillations were propagated from the origin of the noise to the center. In addition, the oscillations also propagated outwards. Thus noise filtering should be considered when the method is applied to the experimental data.

To further validate the noise filtering property, the intensity data calculated from Eq. (15) were added normally distributed random noise with a standard deviation $S = 0.005$ and applied to the two methods. The results are shown in Fig. 5(b). In the inversion of the FH method noise is almost completely suppressed due to the excellent smoothing property with a small

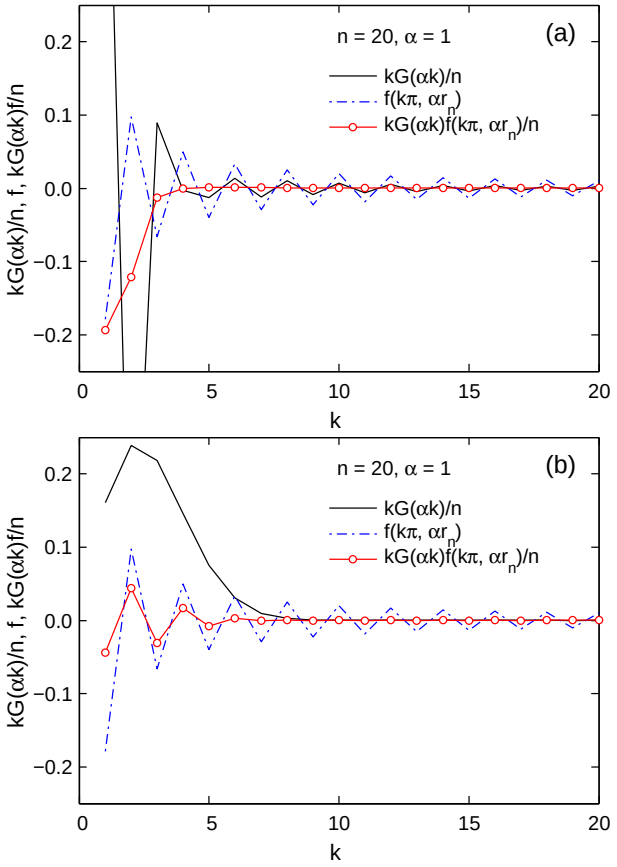

Fig. 4. Variations of $kG(\alpha k)/n$, $f(k\pi,\alpha r_n)$ and their product $kG(\alpha k)f(k\pi,\alpha r_n)/n$ as functions of k calculated using the intensity data in (a) Eq. (13) with off-axis peaks, and (b) Eq. (15) with a Gaussian type.

value of α, while the profile obtained with the FE method is evidently affected by the noise that is greatly magnified especially at the position near the center of the source. Note that if we use a relatively small α to perform the inversion with the FE method, the result will be similar to that inverted with the FH method. Therefore, by decreasing the inversion accuracy (with a lower value of α), the noise resistent properties of the two methods can be improved. There is no doubt that a more accurate method is always more sensitive to noise and thus yields a worse result when the data to be inverted contain noise.

5. Modified Fourier–Hankel method

Considering the contradiction between the performances of accuracy and stability, for both of the methods the value of α should be appropriately lowered to ensure the smoothing property. The FE method seems more desirable as α can be adjusted in a more extensive area to control the degree of smoothing, but due to the oscillation and singularity of the function in the integral of $g(\omega,r)$, the inversion matrix in Eq. (3) is difficult to calculate for data with a large number of points. The FH method, however, cannot achieve a high accuracy especially for small sets of data.

It is worth noting that the FH method with the smoothing factor α is equivalent to the Fourier–Hankel transform in Eq. (9) being discretized for a source with the radius R being extended to R/α and with the high frequencies of the Fourier transform of the projected intensities being dropped. Thus it is desirable to modify the FH method as

$$\varepsilon(r_i) = \frac{\alpha^2\pi}{2nR}\sum_{j=-n}^{n-1} I(x_j)\sum_{k=1}^{\lfloor n/\alpha\rfloor} k\,J_0\left(\frac{\alpha ik\pi}{n}\right)\cos\left(\frac{\alpha jk\pi}{n}\right), \qquad (23)$$

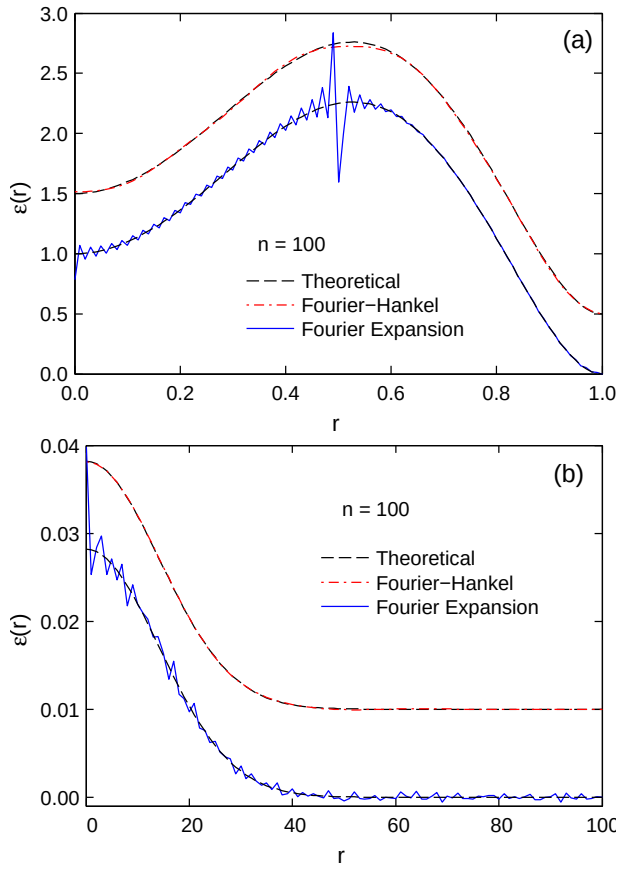

Fig. 5. Comparison of distributions of the theoretical emission coefficients and the values inverted using the FE and FH methods with (a) the value of $I_1(1/2)$ decreased to $0.95I_1(1/2)$ to simulate the noise in the experimental data, and (b) intensities of $I_2(x)$ added normally distributed random noise with a standard deviation $S = 0.005$. The values of α for the FE and FH methods are, 1 and 0.1, respectively. Results of the FH method are offset from the original positions for clarity.

where $\lfloor x \rfloor$ denotes the nearest integer less than or equal to x. The change of the upper limit of the second summation ensures that the truncation error is small for data with very limited points. The value of α should be small enough to ensure that the error owing to the difference between $g(\omega, r)$ and $J_0(\omega r)$ is negligible, as shown in Fig. 2.

The modified Fourier–Hankel (MFH) method was tested with a small set of data calculated from Eq. (13). Fig. 6 shows the results inverted with the FH method and the modified form of Eq. (23). The emission coefficients obtained with the FH method were greatly distorted due to the over-smoothing of noise with too small a value of α, while the MFH method successfully reconstructed the original emission distribution with very small errors. Note that $\alpha = 0.1$ was chosen for the inversion. This small value of α leads to a negligible difference between $g(\omega, r)$ and $J_0(\omega r)$. At the same time, the Fourier components $n+1 \sim \lfloor n/\alpha \rfloor$ were reserved, which ensures that the intensity profile can be more accurately approximated with the cosine basis functions. Thus the modified method can achieve a very high accuracy even for such sparse data.

The modified method was also tested using the functions [10]

$$\varepsilon_k(r) = (1 - r^2)^k, \quad 0 \leqslant r \leqslant 1. \tag{24}$$

Some of these functions with k varying from 1 to 20 are shown in Fig. 7. Standard deviations of the inversion for these functions were calculated for the new algorithm and the FE and FH methods. The results are listed in Table 1. It is clear that the

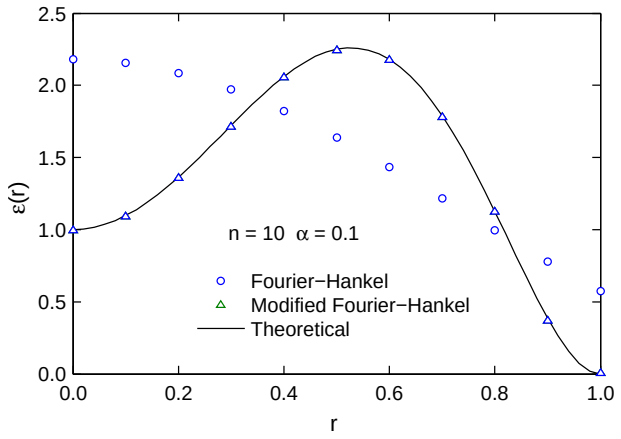

Fig. 6. Comparison of distributions of the theoretical emission coefficients and the values inverted with the FH method and its modified form Eq. (23).

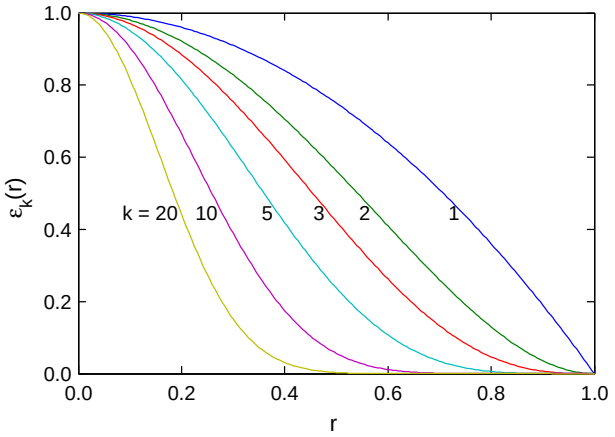

Fig. 7. Distribution of functions $\varepsilon_k(r) = (1 - r^2)^k$ for a range of k.

result of the FH method is the worst. But for $k \leqslant 5$, the MFH method is even more accurate than the FE method. This is because the truncation error of the MFH method is smaller than that of the FE method. When the value of k becomes larger, the derivative at the boundary of the function $\varepsilon_k(r)$ decreases and the truncation error becomes smaller. Therefore, wth the increase of k, the inversion error for all the methods decreases. Besides the truncation error, the MFH method has another error due to the difference between $g(\omega, r)$ and $J_0(\omega r)$, which is relatively small as $\alpha = 0.01$ was chosen. This error limits the accuracy in which the MFH can be achieved, so for large k the FE method is a little superior. Such errors in the FH method can be reduced with a small value of α which, however, will rapidly increase the truncation error.

From these examples it is seen that the modified algorithm indeed greatly reduced the errors that are dominant in the FH method. The MFH method is not only accurate either for large or small sets of data, but also fast and easy to calculate, and the smoothing procedure can be implemented in the reconstruction, which makes the inversion process even faster. Therefore, it is desirable to replace the FE and FH methods with the MFH method for data inversion.

6. Conclusions

Accuracies of the discrete FE and FH methods have been compared and analyzed. The FE method is very accurate even for a small set of data, while the FH method appears to have systematic negative errors. Both matrix forms of the methods have errors caused by the discretization of the continuous Fourier transform and the truncation of the series expansion. In most

Table 1
Comparison of standard deviations σ for the reconstruction of functions $\varepsilon_k(r) = (1-r^2)^k$ for different k using the Fourier expansion, Fourier–Hankel, and modified Fourier–Hankel methods.

	Fourier Expansion	Fourier–Hankel	Modified Fourier–Hankel
k	$\alpha = 1$	$\alpha = 1$	$\alpha = 0.01$
1	1.09E-02	2.83E-01	5.71E-03
2	9.98E-04	1.75E-01	4.37E-04
3	2.54E-04	1.26E-01	5.21E-05
5	2.23E-05	8.15E-02	7.00E-06
10	6.29E-07	4.31E-02	3.73E-06
20	1.14E-07	2.22E-02	1.96E-06

cases, the former is negligible and the latter is important only for inversion with very limited data points. For the FH method, however, the significant error is due to the difference between the functions $g(\omega, r)$ and $J_0(\omega r)$. For large sets of data the inversion error of the FH method can be reduced by adjusting the smoothing factor α to a small value, i.e., increasing the radius of the source. However, for poorly sampled data, this will potentially distort the original distribution of the intensities and thus increases the inversion error.

Though the FE method has a high accuracy, it is very sensitive to noise and the inversion matrix is difficult to calculate, which restrict its application; a smoothing procedure must be implemented when it has been used. The FH method can only be considered when applying it to data with a large number of points by using a small value of α. Considering the weak points of the two methods, a modified Fourier–Hankel method has been proposed, which is accurate, computationally efficient and easy to control the smoothing degree of noise in the inversion.

References

[1] S. Ma, H. Gao, L. Wu, Modified Fourier-Hankel method based on analysis of errors in Abel inversion using Fourier transform techniques, Appl. Opt. 47 (9) (2008) 1350–1357.

[2] H. R. Griem, Principles of Plasma Spectroscopy, Cambridge University Press, Cambridge, 1997.

[3] A. C. Eckbreth, Laser diagnostics for combustion temperature and species, 2nd Edition, Vol. 3 of Combustion Science and Technology Book Series, Gordon & Breach, Amsterdam, 1996.

[4] J. Glasser, J. Chapelle, J. C. Boettner, Abel inversion applied to plasma spectroscopy: a new interactive method, Appl. Opt. 17 (1978) 3750–3754.

[5] Yu. E. Voskoboinikov, N. G. Preobrazhenskii, Abel inversion with high accuracy in the problems of optics and spectroscopy, Opt. Spectrosc. 60 (1986) 111–113.

[6] G. N. Minerbo, M. E. Levy, Inversion of Abel's integral equation by means of orthogonal polynomials, SIAM J. Numer. Anal. 6 (1969) 598–616.

[7] C. J. Cremers, R. C. Birkebak, Application of the Abel integral equation to spectrographic data, Appl. Opt. 5 (1966) 1057–1064.

[8] S. L. Ma, H. M. Gao, G. J. Zhang, L. Wu, Abel inversion using Legendre wavelets expansion, J. Quant. Spectrosc. Radiat. Transfer 107 (2007) 61–71.

[9] K. Tatekura, Determination of the index profile of optical fibers from transverse interferograms using Fourier theory, Appl. Opt. 22 (1983) 460–463.

[10] M. Kalal, K. A. Nugent, Abel inversion using fast Fourier transforms, Appl. Opt. 27 (1988) 1956–1959.

[11] L. M. Smith, D. R. Keefer, S. I. Sudharsanan, Abel inversion using transform techniques, J. Quant. Spectrosc. Radiat. Transfer 39 (1988) 367–373.

[12] J. Dong, R. J. Kearney, Symmtrizing, filtering and Abel inversion using Fourier transform techniques, J. Quant. Spectrosc. Radiat. Transfer 46 (1991) 141–149.

[13] M. J. Buie, J. T. P. Pender, J. P. Holloway, T. Vincent, P. L. G. Ventzek, M. L. Brake, Abel's inversion applied to experimental spectroscopic data with off axis peaks, J. Quant. Spectrosc. Radiat. Transfer 55 (1996) 231–243.

[14] R. Álvarez, A. Rodero, M. C. Quintero, An Abel inversion method for radially resolved measurements in the axial injection torch, Spectrochim. Acta Part B 57 (2002) 1665–1680.

[15] A. Sáinz, A. Díaz, D. Casas, M. Pineda, F. Cubillo, M. D. Calzada, Abel inversion applied to a small set of emission data from a microwave plasma, Appl. Spectrosc. 60 (3) (2006) 229–236.

[16] V. Dribinski, A. Ossadtchi, V. A. Mandelshtam, H. Reisler, Reconstruction of Abel-transformable images: the Gaussian basis-set expansion Abel transform method, Rev. Sci. Instrum. 73 (2002) 2634–2642.

[17] B. J. Whitaker, Imaging in Molecular Dynamics, Cambridge University Press, Cambridge, 2003.

[18] G. N. Watson, Theory of Bessel Functions, Cambridge University Press, New York, 1966.

[19] D. H. Manzella, F. M. Curran, R. M. Myers, D. M. Zube, Preliminary plume characteristics of an arcjet thruster, Tech. Rep. NASA Technical Memorandum 103241, AIAA-90-2645 (1990).

[20] S. M. Candel, An algorithm for the Fourier-Bessel transform, Comp. Phys. Commun. 23 (4) (1981) 343–353.

[21] A. V. Oppenheim, A. S. Willsky, S. H. Nawab, Signals and Systems, Prentice Hall, Englewood Cliffs, NJ, 1996.